Preparation and microwave absorption properties of pitch carbon coating FeNi/ Fe_3O_4 particles

Q. ZHANG[a], Y. LIU[a], X. GAO[a,*], K. ZHANG[a], X. CHEN[b]
[a]*Shi Jia Zhuang Mechanical Engineering College, Shi Jia Zhuang 050003, PR China*
[b]*School of Science, Northwestern Polytechnical University, Xi´an 710072, PR China*

Using petroleum pitch as carbon sources，pitch carbon coating FeNi/Fe_3O_4 particles with 20wt%, 30wt%, 40 wt% carbon were separately prepared by a liquid phase method. Their structures, morphology and microwave absorption properties were investigated and the impacts of the carbon content on the electromagnetic properties were discussed in the frequency ranges of 2–8 GHz. It can be demonstrated that the composites exhibit superior microwave absorption performance in low frequency and the microwave absorption properties of composites decrease with the increasing carbon content from 20 to 40 wt %.For the composites with 20wt% carbon, the maximum RL reaches −26.9 dB at 3.4 GHz with a matching thickness of 5mm and the absorption bandwidths exceeding -10dB are more than 5.2GHz (from the 2.6 to 8GHz) with the thickness of 2-5mm.

(Received August 25, 2018; accepted June 14, 2019)

Keywords: Pitch carbon, Magnetic particles, Composite, Microwave absorber

1. Introduction

In recent years, the microwave absorbing materials have attracted more and more attention due to their important applications in civil and military fields [1-3]. An ideal microwave absorbing material should be lightweight and exhibit high absorption efficiency in a broad frequency band at a low filler loading ratio [4-6]. However, a single material commonly has difficulty in affording thin, light, wideband absorbing properties [7-9]. Accordingly, significant efforts have been devoted to the development of microwave absorbing composites. As we know, the microwave absorption capacity is mainly determined by the relative permittivity (ε_r), the relative permeability (μ_r), the electromagnetic (EM) impedance match and the microstructure of the absorber [10]. Carbon-coated magnetic materials can combine the dielectric properties of carbon with the magnetic properties of magnetic materials, so that the composites have better microwave absorption properties [11].

Che and co-workers have reported that magnetic nanoparticles/carbon nanotubes (CNTs) exhibited improved microwave absorption properties because of their proper EM matching between the dielectric loss and the magnetic loss [12,13]. Zhao et al. have fabricated Graphene (G)-coated Fe nanocomposites and reported that the excellent microwave absorption performance of Fe/G was mainly ascribed to the intrinsic change of dielectric properties [14]. Additionally, Qiang et al. have prepared Fe_3O_4/ Carbon fibers composites with low density, strong and wide frequency microwave absorption [15] .Wang et al. fabricated Graphene (G)–Fe_3O_4 nanohybrids and the maximum reflection loss was up to -40.36dB with a thickness of 5.0mm[16]. Wang et al. synthesized Fe_3O_4/Graphene and Ni/Graphene composites by an atomic layer deposition (ALD) method. And the coated graphene materials exhibited remarkably improved microwave absorption properties compared to the pristine graphene [17].

In this study, pitch carbon coating FeNi/Fe_3O_4 particles were synthesized for the first time. And the influence of the carbon content on the electromagnetic properties was analyzed in the frequency range of 2–8 GHz.

2. Experiment procedure

2.1. Materials

FeNi/Fe_3O_4 particles (the proportion of the FeNi and Fe_3O_4 was 3:1) were provided by Guangzhou Jinnan Magnetic Plastic (Co., LTD, China),which were used directly without further purification. Petroleum pitch were purchased from Baoding Petroleum Asphalt (Co., LTD, China). All other materials were of analytical grade and commercially available.

2.2. Synthesis of pitch carbon@ FeNi/ Fe_3O_4 composites through liquid phase method

Three sets of samples with different carbon content

were prepared as follows: In brief, 4.0 g of petroleum pitch was first dissolved in 200ml kerosene solution. After being stirred for 1h, the solution was filtered to remove insoluble substance to obtain kerosene solution of pitch (0.02g/ml, 200ml). 1.5 g of magnetic particles(FeNi/ Fe_3O_4) were separately added to 19 ml, 32 ml, 50 ml of the above kerosene solution of pitch(0.02g/ml).The above mentioned mixed solution was ultrasonicated for 5h and then stirred for 2 h at 80℃ to evaporate the kerosene solvent, then the products were vacuum-dired at 70℃ for 12h. Finally, the black products were transferred to a tube furnace and heated to 750℃ with a rate of 10 ℃/min, and then the products were held at 750℃ for 3h in flowing Ar. After that, the products were cooled to room temperature naturally in flowing Ar. The finally synthesized products were separately named SP-1(20wt% carbon), SP-2(30% carbon), SP-3(40% carbon).

2.3. Characterization and measurement

The structure of the composites was investigated by power X-ray diffraction (XRD) with Cu-Ka radiation at 40KV and using 100mA. Raman spectrum was performed on a Raman microscope equipped with a 514 nm laser. The morphology of the composites was observed by a scanning electron microscope (FE-SEM, S-4800, Hitachi). The relative complex permittivity (ε_r) and permeability (μ_r) were measured by a HP8753D vector network analyzer in the frequency range of 2−8 GHz. The test samples were composed of pitch carbon@ FeNi/ Fe_3O_4 and paraffin, which were processed to form a toroidal shaped samples with an outer diameter of 7.0mm, inner diameter of 3.04mm and height of about 3.0mm.

3. Results and discussions

3.1. Structural properties

Fig. 1 (a) shows the XRD patterns of pitch carbon @FeNi/Fe_3O_4 composites. It can be seen that the three groups of samples show obvious diffraction peaks at 2θ = 43.6 °, 50.8 ° and 74.7 °, corresponding to the (111), (200), (220) planes of FeNi (JCPDF12-0736). And the diffraction peaks can also be observed at 2θ = 30.2 °, 35.6 °, 43.0 ° 53.4 °, 57.6 ° and 63.2 °, corresponding to the（220），(311),(400),(422),(511), （ 440 ） planes of Fe_3O_4 (JC PDF99-0073). Signals of pitch carbon can hardly be detected from the Fig. 1 (a), due to the weaker scattering power of carbon compared with the magnetic particles. Nevertheless, pitch carbon in the samples can be readily identified by Raman spectroscopy Fig. 1 (b). As shown in Figure 1b, two strong peaks appeared at 1329cm^{-1} and 1576 cm^{-1}, which were known as the D peak and G peak, respectively [18]. The D peak could be attributed to the breathing mode of C-SP^2 atoms in rings and related with defects and disorder in the structure, while G peak is mainly assigned to the vibration of sp^2 bonded carbon atoms. Moreover, the D peak position is slightly shifted towards a lower frequency than that of bulk diamond (1332 cm^{-1}). This is attributed to the phonon confinement effects resulting from mass aberrance in the graphite atom layers. In addition, the G peak was also located at a lower frequency compared with bulk graphite (1580 cm^{-1}). This is thought to be due to the strain and unevenness of the curving graphite layers [19]. In addition, the values of ID/IG reflected disorder degree. Clearly, the value of ID/IG became lower with the increase content of the magnetic FeNi/ Fe_3O_4 particles.

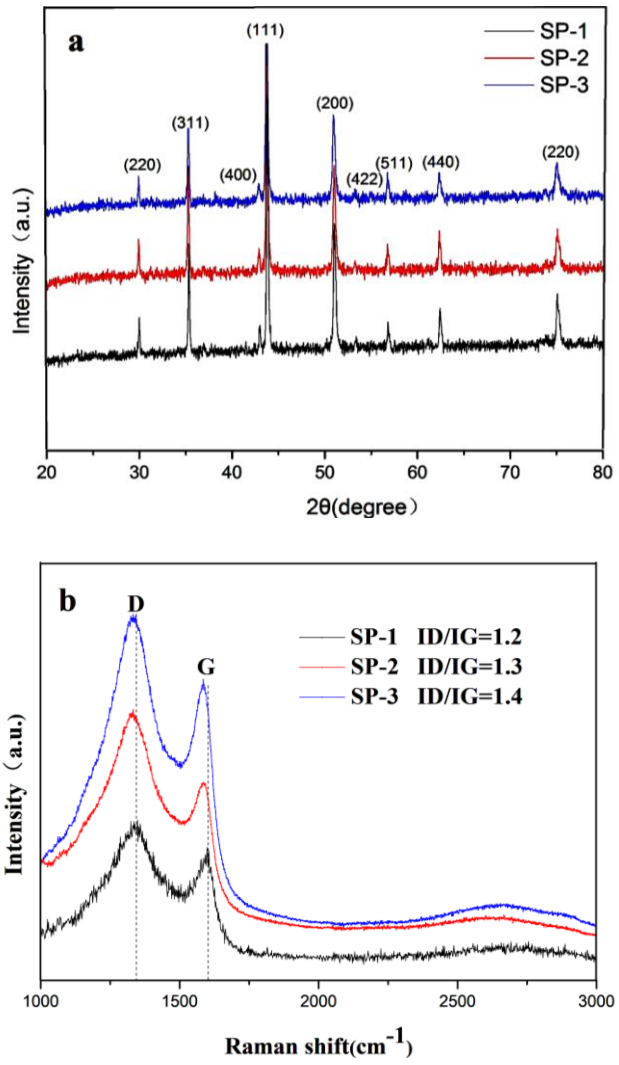

Fig. 1. (a) X-ray diffraction pattern and (b) Raman shift of the pitch cabon @FeNi/Fe_3O_4

3.2. Morphology analysis

Fig. 2 shows the SEM images of pitch cabon @FeNi/Fe_3O_4. As shown in Fig. 2 (a) and (b), the pitch carbon and the magnetic particles (FeNi/Fe_3O_4) can be observed obviously. The partial enlarged image of the composite were given in Fig. 2 (c) and (d) .

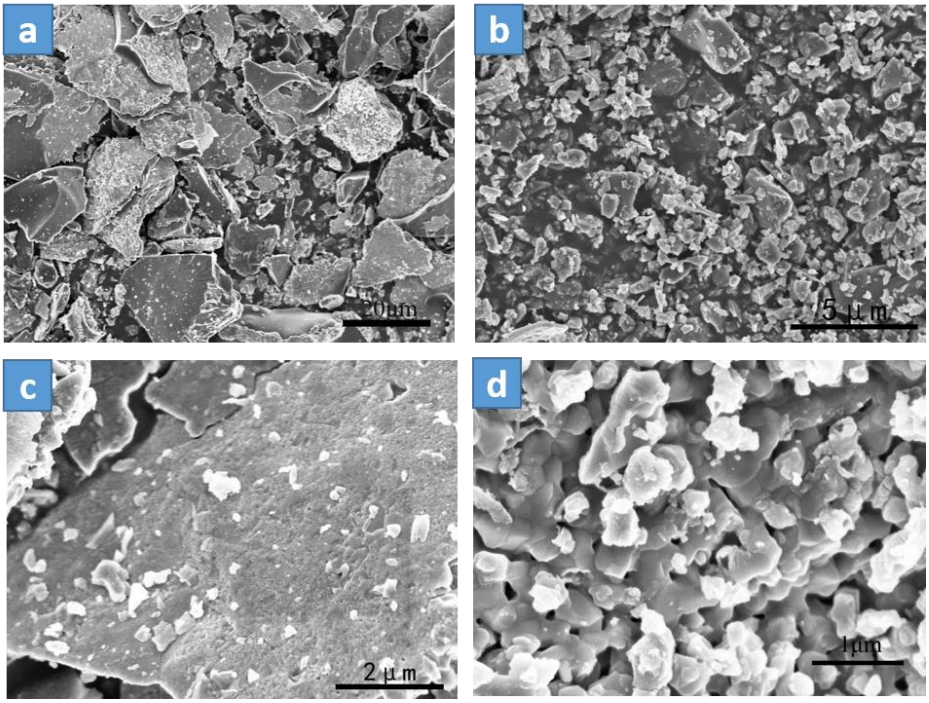

Fig. 2. SEM images of the pitch cabon @FeNi/Fe_3O_4

It can be seen that the magnetic particles were evenly attached to the carbon skeleton and the grain size of magnetic particles ranges from 0.2μm to 0.6μm. Meanwhile, there are some defects on the surface of pitch carbon.

3.3. Microwave absorption properties

Fig. 3 shows the real part (ε′) and imaginary part (ε′′) of the permittivity for the three samples in the range of 2-8 GHz, respectively. The ε′ is mainly associated with the amount of polarization occurring in the materials .And the ε′′ is mainly related to the electronic conductivity of materials [20,21]. As shown in Fig. 3, the ε′ value of SP-1is about 12.5 and almost independence on frequency, while the ε′ value of SP-2 and SP-3 is 16.6-14.0 and 26.1-21.2, exhibiting a small fluctuation, respectively. In addition, the ε′′ of three samples all show a fluctuation over the 2-8GHz. And the value of ε′′ for SP-1, SP-2 and SP-3 is 0.8-1.6,1.8-3.5, and 3.0-7.7, respectively. It can be found that both ε′ and ε′′ values increase with the increasing carbon content. For impedance match, a too high value of permittivity is disadvantageous and may cause strong reflection and weak absorption[22].Thus, SP-1and SP-2 with a relatireal part of permittivity may achieve good impedance match .While, the ε′′ value of SP-3 is larger than that of SP-2 and SP-3, indicating an increased dielectric loss.

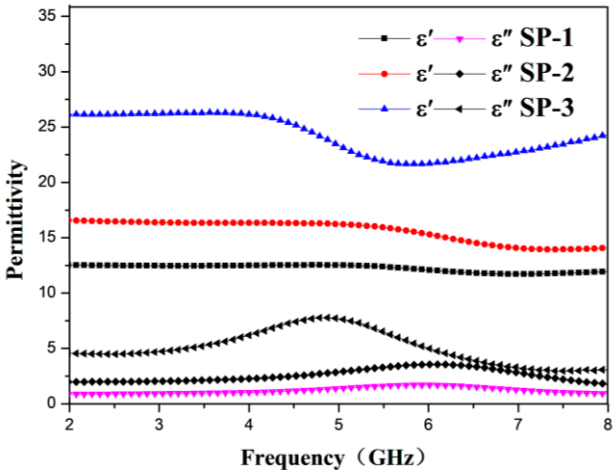

Fig. 3. Frequency dependence of relative permittivity

Fig. 4 shows the frequency dependence of real part (μ′) and imaginary part (μ′′) of magnetic permeability for the three samples in the range of 2-8 GHz. The values of μ′ for three samples are almost same and decrease from around 1.75 to 0.9 with the increasing frequency. And the values of μ′′ for three samples exhibit a similar trend from around 0.77 to 0.6. Unlike the dielectric behavior, there are no significant changes of permeability properties with the increasing of carbon content, indicating a small difference of magnetic loss between three samples.

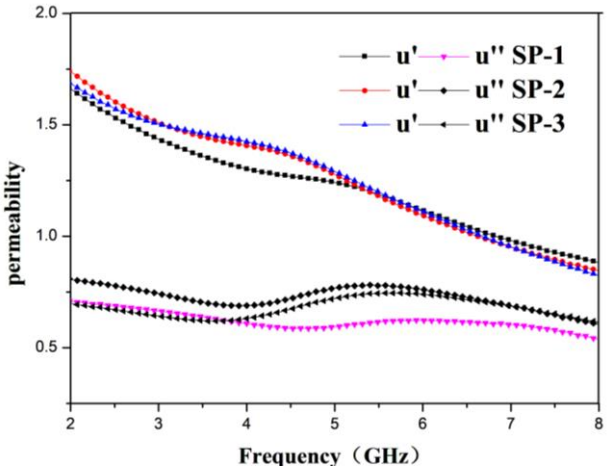

Fig. 4. Frequency dependence of relative permeability

Based on the data of permittivity and permeability, the reflection loss (RL) of three samples were calculated according to the transmission line theory [23]:

$$RL\ (\mathrm{dB}) = 20\log\left|\frac{Zin-1}{Zin+1}\right| \quad (1)$$

$$Zin = \sqrt{\mu_r/\varepsilon_r}\tanh\left[j(2\pi fd/c)\sqrt{\varepsilon_r\mu_r}\right] \quad (2)$$

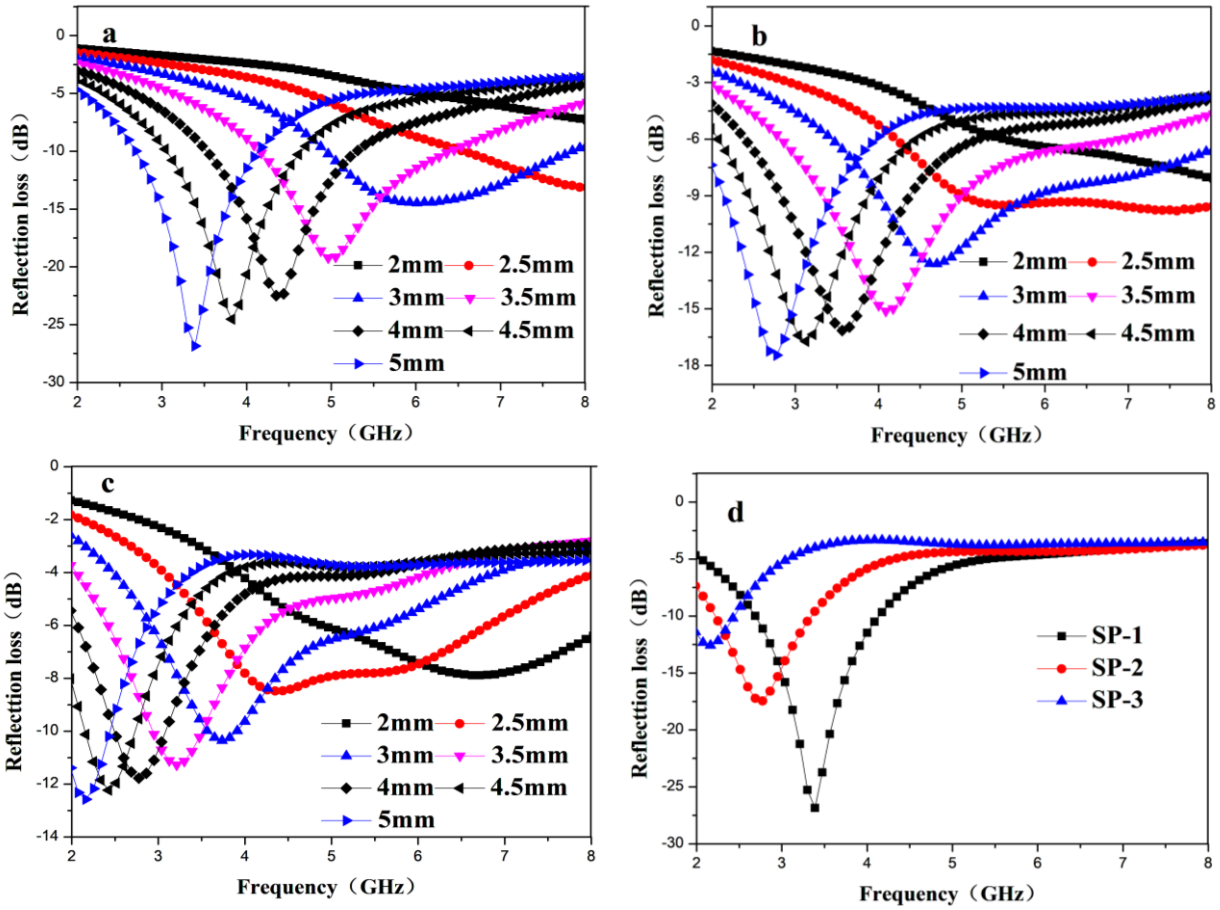

Fig. 5. The reflection loss of the synthesized samples

As illustrated in Fig. 5 (a), the peak values of RL for SP-1 are all less than -10 dB and shift to lower frequency with the thickness ranging from 2mm to 5mm. The maximum RL reaches −26.9 dB at 3.4 GHz with a matching thickness of 5mm and the absorption bandwidths exceeding -10dB are more than5.2GHz (from the 2.6 to 8GHz) with the thickness of 2-5mm.In addition, the effective bandwidth (the frequency range in which RL is less than-10 dB) of SP-1 reaches the maximum of 2.8 GHz with the thickness of 3 mm. For SP-2 in Fig. 5(b), it can be found that SP-2 also exhibits excellent microwave absorption performance in 2-8GHz as the same as SP-1. The maximum RL is about −17.4dB and its matching frequency is 2.8 GHz and the corresponding value of matching thickness is 5 mm. It is noted that the values of RL less than −10dB are obtained over the range of

2.2-8GHz with an absorber thickness of 2–5 mm. Compared with SP-1 and SP-2, SP-3 shows weaker microwave absorption ability as shown in Fig. 5 (c). The maximum RL of SP-3 is up to -12.58 dB at 2.2 GHz with a thickness of 5mm. Fig. 5 d gives the maximum RL of three samples, it can be found that the maximum RL of SP-1 is more large than that of SP-2 and SP-3 .On the basis of above discussion, It is clearly that the pitch carbon coating $FeNi/Fe_3O_4$ particles exhibit remarkable microwave absorption properties in low-frequency.

And SP-1(20 wt% carbon) has the most excellent microwave absorption properties among the three samples. It can be demonstrated that microwave absorption properties of pitch carbon coating $FeNi/Fe_3O_4$ particles decrease with the increasing carbon content from 20 to 40 wt %.

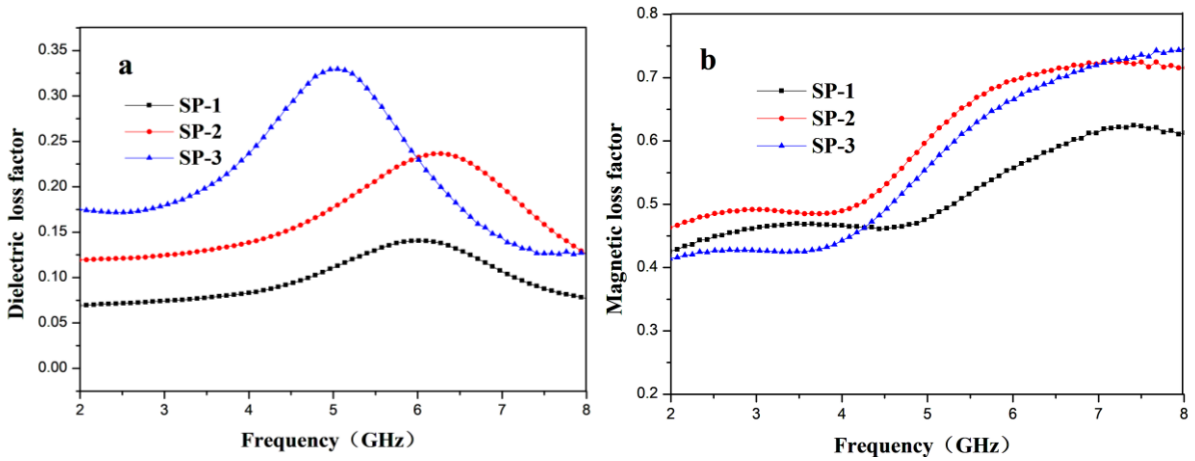

Fig. 6. (a) Dielectric loss factor and (b) magnetic loss factor of three samples

The dielectric loss factor ($\tan\delta\varepsilon = \varepsilon'' / \varepsilon'$) and the magnetic loss factor ($\tan\delta\mu = \mu'' / \mu'$) may well explain why the composites have more excellent microwave absorption properties, as shown in figure.6. It can be found that the values of magnetic loss factor for three samples are from around 0.4 to 0.75 and the values of dielectric loss factor are from around 0.06 to 0.33, the complementarities between dielectric loss and magnetic loss which originate from the pitch carbon and $FeNi/Fe_3O_4$ particles, respectively, would be helpful to the enhanced microwave absorption properties of the composites. And it is observed that the dielectric loss factor of SP-1 is more steady than other samples and shows a value around 0.06 to 0.14with slight fluctuation, whereas the values of the magnetic loss factor for SP-1 gradually increase from 0.4 to 0.6 over the 2–8 GHz range. The steady dielectric loss of SP-1 is helpful to obtain a good impedance matching condition so that it is more favorable for the dissipation of microwave energy.

4. Conclusions

In summary, in this work, pitch carbon coating $FeNi/Fe_3O_4$ particles with 20wt%, 30wt%, 40wt% carbon were fabricated by a liquid phase method , respectively. Their structures and morphology were investigated by XRD, Raman and SEM in detail. For SP-1, SP-2 and SP-3, the microwave absorption properties and the influence of the carbon content on the electromagnetic properties were discussed. The experimental results indicate that the pitch carbon coating $FeNi/Fe_3O_4$ particles exhibit superior electromagnetic wave absorption performance in 2-8GHz.The SP-1(20wt% carbon) has the maximum reflection loss of −26.9 dB at 3.4 GHz and an effective bandwidth of 2.8 GHz. In addition, the microwave absorption properties of pitch carbon coating $FeNi/Fe_3O_4$ particles decrease with the increasing carbon content from 20 to 40 wt %. we think the pitch carbon coating $FeNi/Fe_3O_4$ composites are promising electromagnetic wave absorbers in low-frequency.

References

[1] W.-L.Song, M.-S. Cao, L.-Z. Fan et al., Carbon **77**, 130 (2014).
[2] Y.-F. Wang, D.-L. Chen, X. Yin et al., ACS Appl. Mater. Interfaces**7**(47), 26226 (2015).
[3] X.- F. Chen, Y. Huang, K.- C. Zhang, Journal of Colloid and Interface Science **513**, 788 (2018).
[4] G. - L. Wu, Z.- R. Jia, Y.- H. Cheng et al., Applied Surface Science. **464**, 472 (2019).
[5] F. Wu, A. Xie, M. Sun et al., J. Mater. Chem. **3**, 14358 (2015).
[6] X. - F. Chen, Y. Huang, K.-C. Zhang et al., Electrochimica Acta. **259**, 131 (2018).
[7] G. – L. Wu, Y. - H. Cheng, Z. - H. Yang et al., Chemical Engineering Journal. **333**, 519 (2018).
[8] P.- B. Liu,, M.- Y. Yang, S.- H. Zhou et al., Electrochimica Acta. **294**, 383 (2019).
[9] G. - L. Wu, H.-X. Zhang, X. - X. Luo et al., Journal

of Colloid and Interface Science. **536**, 548 (2019).
[10] P. - B. Liu, Y. - D. Zhu, X.-G. Gao et al., Chemical Engineering Journal **350**, 79 (2018).
[11] P. - B. Liu, J. Yan, X.-G. Gao et al., Electrochimica Acta **272**, 77 (2018).
[12] R.-C. Che, L. - M. Peng, X. - F. Duan et al., Adv. Mater. **16**, 401 (2004).
[13] R.-C. Che, C.- Y. Zhi, C.- Y. Liang et al., Appl. Phys. Lett. **88**, 033105 (2006).
[14] X.-C. Zhao, Z.-M. Zhang, L.-Y. Wang et al., Sci. Rep. **3**, 3421 (2013).
[15] C.-W. Qiang, J.-C. Xua, Z.-Q. Zhang et al., Journal of Alloys and Compounds **506**, 93 (2010).
[16] T.-S. Wang, Z.-H. Liu, M.-M. Lu et al., J. Appl. Phys. **113**, 024314 (2013).
[17] G.-Z. Wang, Z. Gao, G.-P. Wan et al., Nano Research. **7**(5), 704 (2014).
[18] X.- F. Zhang, X.- L. Dong, H. Huang et al., J. Phys. D Appl. Phys. **40**, 5383 (2007).
[19] D. Roy, M. Chhowalla, H. Wang, Chem. Phys. Lett. **373**, 52 (2003).
[20] Y. Zhang, A. Zhang, L. Ding et al., Appl. Sci. Manuf. **81**, 264 (2016).
[21] K.-C. Zhang, X.-B. Gao, Q. Zhang et al., J. Mater. Sci.: Mater Electron. **28**, 1352 (2017).
[22] L. Wang, Y. Huang, C. Li et al., Phys. Chem. Chem. Phys. **17**(3), 2228 (2015).
[23] F. Qin, H. X. Peng, Prog. Mater. Sci. **58**, 183 (2013).

*Corresponding author: xbgaotg@126.com